PCP
PLANT & CELL PHYSIOLOGY

Plastidial Folate Prevents Starch Biosynthesis Triggered by Sugar Influx into Non-Photosynthetic Plastids of Arabidopsis

Makoto Hayashi[1,*], Mina Tanaka[2], Saki Yamamoto[1], Taro Nakagawa[1], Masatake Kanai[2], Aya Anegawa[3,4], Miwa Ohnishi[3], Tetsuro Mimura[3] and Mikio Nishimura[2]

[1]Department of Bioscience, Nagahama Institute of Bioscience and Technology, Tamura 1266, Nagahama, Shiga 526-0829, Japan
[2]Department of Cell Biology, National Institute for Basic Biology, Okazaki 444-8585, Japan
[3]Department of Biology, Graduate School of Science, Kobe University, Rokkodai 1-1, Nada-ku, 657-8501, Japan
[4]Present address: Agilent Technologies Japan, Ltd., Hachioji, Tokyo 192-8510, Japan.
*Corresponding author: E-mail,: makoto_hayashi@nagahama-i-bio.ac.jp; Fax, +81-749-64-8101.
(Received February 28, 2017; Accepted May 16, 2017)

Regular Paper

Regulation of sucrose–starch interconversion in plants is important to maintain energy supplies necessary for viability and growth. Arabidopsis mutants were screened for aberrant responses to sucrose to identify candidates with a defect in the regulation of starch biosynthesis. One such mutant, *fpgs1-4*, accumulated substantial amounts of starch in non-photosynthetic cells. Dark-grown mutant seedlings exhibited shortened hypocotyls and accumulated starch in etioplasts when supplied with exogenous sucrose/glucose. Similar starch accumulation from exogenous sucrose was observed in mutant chloroplasts, when photosynthesis was prevented by organ culture in darkness. Molecular genetic analyses revealed that the mutant was defective in plastidial folylpolyglutamate synthetase, one of the enzymes engaged in folate biosynthesis. Active folate derivatives are important biomolecules that function as cofactors for a variety of enzymes. Exogenously supplied 5-formyl-tetrahydrofolate abrogated the mutant phenotypes, indicating that the *fpgs1-4* mutant produced insufficient folate derivative levels. In addition, the antifolate agents methotrexate and 5-fluorouracil induced starch accumulation from exogenously supplied sucrose in dark-grown seedlings of wild-type Arabidopsis. These results indicate that plastidial folate suppresses starch biosynthesis triggered by sugar influx into non-photosynthetic cells, demonstrating a hitherto unsuspected link between plastidial folate and starch metabolism.

Keywords: Folate metabolism • Folylpolyglutamate synthetase • Plastid • Starch metabolism • Sucrose transport • Sugar uptake.

Abbreviations: ADPG, ADP glucose; AGPase, ADP-glucose pyrophosphorylase; DHF, dihydrofolate; FPGS, folylpolyglutamate synthetase; 5FU, 5-fluorouracil; GFP, green fluorescent protein; G1P, glucose-1-phosphate; G6P, glucose-6-phosphate; PGM, phosphoglucomutase; RT–PCR, reverse transcription–PCR; RuBisCO, ribulose-1,5-bisphosphate carboxylase/oxygenase; SEX4, starch excess 4; SS, starch synthase; TAG, triacylglycerol; THF, tetrahydrofolate; UDPG, UDP glucose.

Introduction

Oilseed plants such as Arabidopsis accumulate triacylglycerol (TAG) lipid reserves in their seeds (Hayashi and Nishimura 2006, Theodoulou and Eastmond 2012). Each cell within a seed contains numerous oil bodies, which are specialized TAG storage organelles. When the seed starts to germinate, TAG lipase on the oil body membrane degrades TAG into glycerol and fatty acids (Eastmond 2006). The fatty acids are then imported into the glyoxysome by PED3/CTS/PXA1, an ABC transporter found in the glyoxysomal membrane (Hayashi et al. 2002b), and activated to acyl-CoA by acyl-CoA synthetases (Hayashi et al. 2002a). Acyl-CoA is then catabolized into succinate by two metabolic pathways, namely fatty acid β-oxidation and the glyoxylate cycle (Mori and Nishimura 1989, Hayashi et al. 1995, Kato et al. 1995, Kato et al. 1996, Mano et al. 1996, Hayashi et al. 1998a, Kato et al. 1998, Hayashi et al. 1999, Hayashi et al. 2001). Succinate is converted to sucrose by the successive action of mitochondrial and cytosolic enzymes (Hayashi and Nishimura 2002, Hayashi and Nishimura 2003). Sucrose is utilized for long-distance energy transfer from storage sites to cells requiring energy for growth and division during the early stages of post-germinative development before the onset of photosynthesis. Proper delivery of sucrose to the final destination deeply affects the seedling growth. For example, mutants that have defects in glyoxysomal fatty acid β-oxidation cannot germinate in the absence of sucrose, and require exogenously supplied sucrose for their post-germinative growth (Hayashi et al. 1998b).

Non-photosynthetic cells need to catabolize sucrose rapidly to obtain sufficient energy to support ongoing growth. To investigate the mechanisms underlying sucrose metabolism in non-photosynthetic cells, we screened Arabidopsis mutants that exhibited aberrant responses to sucrose during post-germinative growth in the dark without the action of photosynthesis. One of these mutants, which abnormally accumulated starch in non-photosynthetic cells when sucrose was exogenously supplied, is described in this study. The mutant had a defect in a folate biosynthesis gene that encodes plastidial folylpolyglutamate synthetase (FPGS).

Editor-in-Chief's Choice

Plant Cell Physiol. 58(8): 1328–1338 (2017) doi:10.1093/pcp/pcx076, Advance Access publication on 6 June 2017,
available FREE online at www.pcp.oxfordjournals.org

Folate, also known as vitamin B_9, is an essential cofactor for several metabolic enzymes involved in processes such as nucleotide and amino acid biosynthesis (Ravanel et al. 2011). Although a large variety of folate derivatives have been identified, the biologically active molecules are thought to be tetrahydrofolate (THF) and its C1-substituted derivatives with polyglutamate tails such as formyl-THF(Glu)n, methyl-THF(Glu)n, methenyl-THF(Glu)n and methylene-THF(Glu)n. Plants can synthesize these derivatives de novo, but animals, including humans, cannot, and require dietary sources. The folate biosynthetic pathway has been extensively studied in plants, mainly because of the importance of folate in human nutrition and health (Hanson and Gregory 2011, Gerdes et al. 2012).

THF is first synthesized as dehydrofolate (DHF) through assembly of pterin, *para*-aminobenzoic acid (pABA) and glutamate in mitochondria. THF is produced from DHF by the action of dehydrofolate reductase, and is then distributed to the plastids and cytosol as well as the mitochondria. Each cellular compartment contains a set of enzymes that adds a polyglutamate tail and a C1 unit to THF. Addition of a polyglutamate tail to THF is catalyzed by FPGS. FPGS enzymes in different cellular compartments were identified in Arabidopsis, namely FPGS1 (At5g05980), FPGS2 (Atg310160) and FPGS3 (At3g55630) for the plastidial, cytosolic and mitochondrial isozymes, respectively (Ravanel et al. 2001).

Chemicals that inhibit enzymes involved in folate biosynthesis or that inhibit enzymes requiring folate derivatives as cofactors are called antifolate agents. An example of the former is methotrexate, which inhibits dihydrofolate reductase, and an example of the latter is 5-fluorouracil (5FU), which inhibits thymidylate synthetase (Zhao and Goldman 2003, Kremer 2004). Folate metabolism is an established target for human cancer therapy, and antifolate agents are often used as anticancer drugs. However, despite the importance of folate in animal cells, the physiological roles of folate derivatives in plants remain under investigation (Miret and Munne-Bosch 2014, Colinas and Fitzpatrick 2015).

Here, we present evidence demonstrating a previously unidentified link between folate and starch metabolism, and discuss the physiological functions of plastidial folate in sucrose–starch interconversion in non-photosynthetic cells.

Results

Isolation of a mutant with exogenous-sucrose-dependent starch accumulation

In the course of a screen of ethyl methanesulfonate-mutagenized Arabidopsis to identify mutants with an aberrant response to sucrose, we identified a mutant that exhibited a shortened hypocotyl when grown on sucrose-containing medium in darkness. This mutant was designated *fpgs1-4* (see below for details). The hypocotyl length of the dark-grown seedlings depended on the sucrose concentration in the medium (**Fig. 1A**). When sucrose was absent, the *fpgs1-4* hypocotyl was of similar length to that of wild-type Arabidopsis. However, when *fpgs1-4* was grown on a medium containing >15 mM sucrose, hypocotyl length was significantly shortened and the root did not elongate. In contrast, hypocotyl length in dark-grown wild-type Arabidopsis remained unchanged at all concentrations of sucrose tested (**Fig. 1B**).

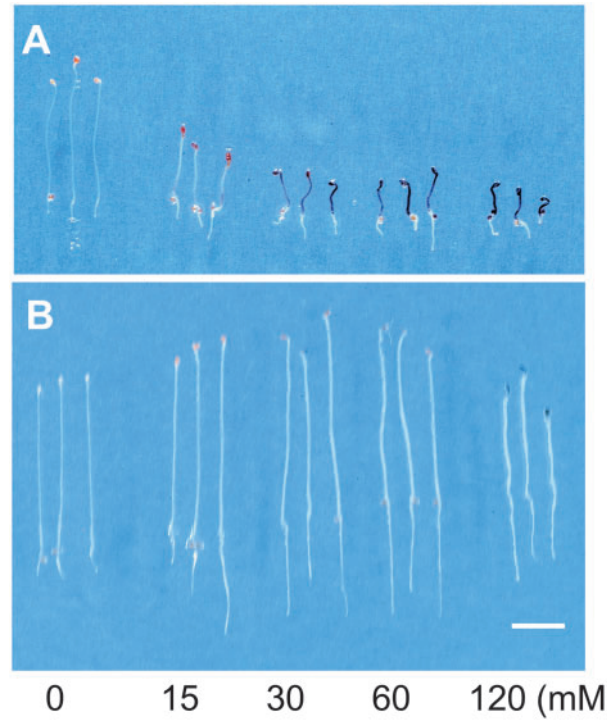

Fig. 1 Etiolated *fpgs1-4* seedlings accumulate starch in a sucrose-dependent manner. Mutant *fpgs1-4* (A) and wild-type (B) Arabidopsis were grown for 5 d in darkness on growth medium containing sucrose. Starch accumulated in seedlings was visualized by iodine staining. Photographs were taken after seedlings were rearranged on agar plates. Sucrose concentrations used for seedling growth are indicated underneath the panel. Scale bar = 5 mm.

Detailed analysis of the phenotype revealed that the dark-grown seedlings of *fpgs1-4* accumulated starch in the presence of sucrose. Starch in seedlings was visualized by iodine staining, as shown in **Fig. 1**. Accumulation of starch in *fpgs1-4* seedlings became apparent in above-ground plant parts (cotyledons and hypocotyl) when seedlings were grown on medium containing >30 mM sucrose (**Fig. 1A**). In contrast, none of the sucrose concentrations tested triggered starch accumulation in wild-type Arabidopsis (**Fig. 1B**). To confirm accumulation of starch in the mutant, starch content was measured in the etiolated seedling and dry seed. The *fpgs1-4* mutant accumulated 1.96 ± 0.14 μg of starch per seedling when grown on medium containing 60 mM sucrose in darkness, whereas wild-type Arabidopsis accumulated 0.25 ± 0.05 μg of starch per seedling in the same conditions. However, when seedlings were grown without sucrose in darkness, both *fpgs1-4* and wild-type Arabidopsis contained very low amounts of starch: 1.6 ± 0.9 and 2.1 ± 0.5 ng of starch per seedling, respectively. Starch content was also determined in dry seed. The *fpgs1-4* mutant and wild-type Arabidopsis contained 1.56 ± 0.05 and 1.03 ± 0.11 ng per seed, respectively, indicating that both the mutant and wild type contained very low amounts of starch. It should be noted that the mutant roots also did not accumulate starch (**Fig. 1A**),

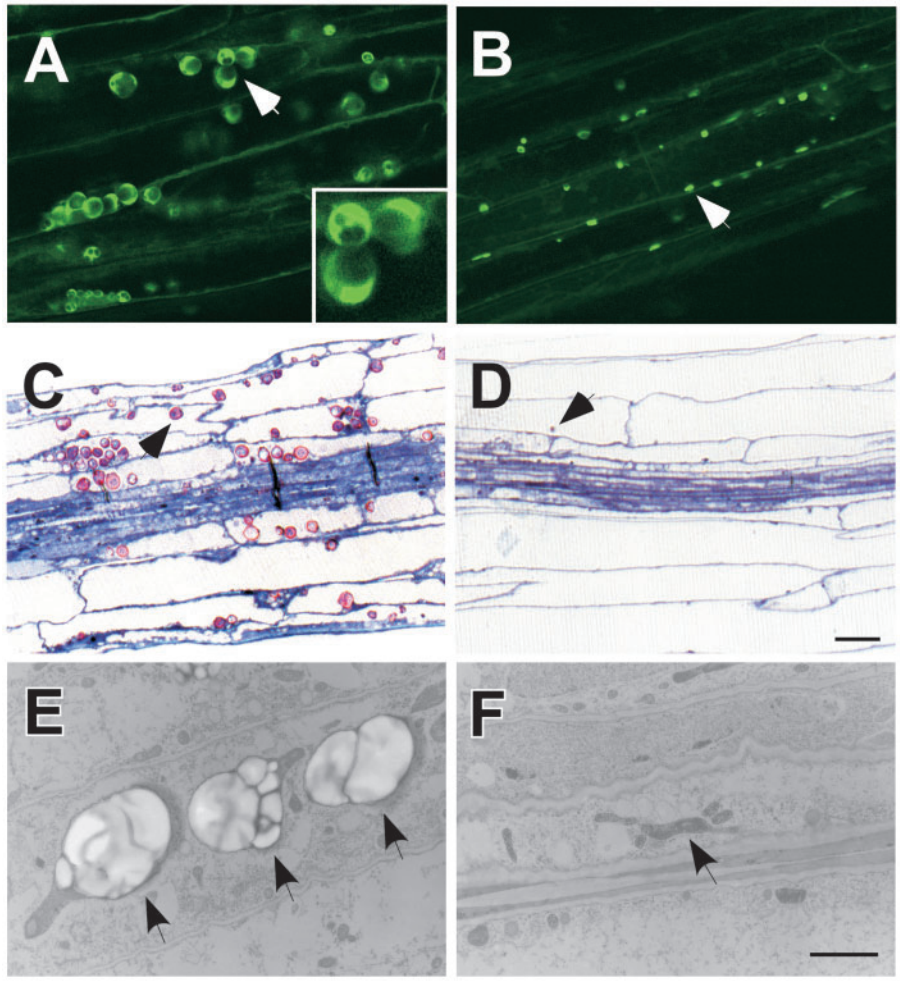

Fig. 2 Morphology of etioplasts in *fpgs1-4* cells. Etiolated seedlings of *fpgs1-4*(cp-GFP) (A), Cp-GFP (B), *fpgs1-4* (C and E) and wild-type Arabidopsis (D and F) were grown for 5 d in darkness on growth medium containing 60 mM sucrose. GFP fluorescence in hypocotyl cells was detected using laser confocal microscopy (A and B). (A) A 2.5-fold enlarged image showing etioplasts, as indicated by the arrow. Thin sections of hypocotyl cells stained with iodine and toluidine blue solutions were observed under light microscopy (C and D). Ultrathin sections were analyzed by electron microscopy (E and F). Arrows indicate plastids. Magnifications in (A–D) and (E–F) are the same. Scale bars in (D) and (F) represent 20 and 0.2 μm, respectively.

Etioplasts of the mutant can produce starch granules

Cells of dark-grown seedlings usually contain etioplasts, a type of differentiated plastid that is not thought to accumulate starch. To analyze the morphology of etioplasts in mutant hypocotyls, *fpgs1-4* was crossed with cp-GFP, an Arabidopsis line that expressed an N-terminal transient peptide of ribulose-1,5-bisphosphate carboxylase/oxygenase (RuBisCO) small subunit plus green fluorescent protein, to produce plastid-localized GFP (Mano et al. 2009). The plant homozygous for both *fpgs1-4* and the transgene was designated as *fpgs1-4*(cp-GFP). As shown in **Fig. 2A**, plastids of up to 10 μm in diameter were detected in *fpgs1-4*(cp-GFP) cells grown in the presence of 60 mM sucrose. These plastids were significantly larger than the etioplasts found in wild-type Arabidopsis, which were approximately 1 μm in diameter (**Fig. 2B**). All the enlarged plastids contained regions that had no GFP fluorescence (see superimposed image in **Fig. 2A**). These regions may correspond to starch granules, which would not be penetrated by cp-GFP.

Thin and ultrathin sections were prepared from *fpgs1-4* and wild-type Arabidopsis seedlings grown on 60 mM sucrose in darkness. The thin sections were stained with iodine and toluidine blue solutions and analyzed using light microscopy. Purple staining, which indicated the presence of starch, was detected in organelles of *fpgs1-4* cells but not wild-type cells (**Fig. 2C, D**). The stained *fpgs1-4* organelles were similar in size to the enlarged plastids detected in *fpgs1-4*(cp-GFP) (**Fig. 2A**). Ultrathin sections were analyzed by electron microscopy. Starch granules were found in enlarged etioplasts in *fpgs1-4* cells (**Fig. 2E**), but not in etioplasts in wild-type Arabidopsis cells (**Fig. 2F**).

Identification of *FPGS1*

The mutant *fpgs1-4*, which had a Columbia background, was outcrossed to wild-type Arabidopsis accession Landsberg *erecta*. F_2 progeny (277 progeny; 554 chromosomes) exhibiting

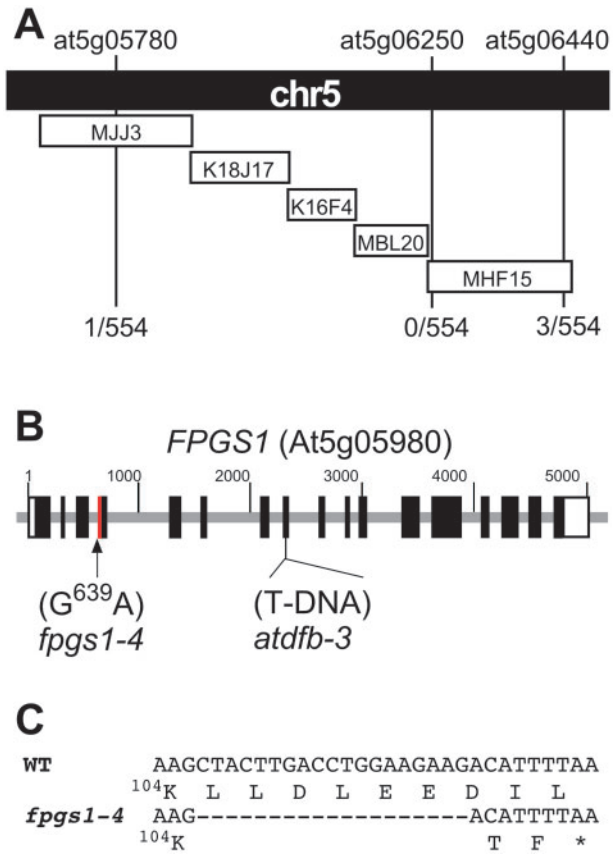

Fig. 3 Positional cloning of the mutated gene. (A) High-resolution mapping of the gene responsible for the mutant phenotype. The gene was mapped to chromosome 5. The names and positions of the molecular markers used for mapping are indicated at the top of the illustration. The number of recombination events occurring in 277 F_2 progeny (554 chromosomes) between the gene locus and the molecular marker are shown below the diagram. Open bars represent the region spanned by the indicated BAC (baterial artificial chromosome) clones. (B) Schematic diagram of At5g05980. Exons are indicated by black boxes, and 5′- and 3′-non-coding regions are illustrated with white boxes. The arrow indicates a single nucleotide substitution of guanine to adenine at the end of the third intron in the *fpgs1-4* allele. T-DNA indicates the position of the T-DNA insertion in the *atdfb-3* allele (SALK_015472). (C) Comparison of cDNA and amino acid sequences between wild-type Arabidopsis (WT) and *fpgs1-4*. Partial cDNA sequences from the end of the third exon and the beginning of the fourth exon are shown together with their translation products. Dashes and asterisks represent deletions and a stop codon, respectively.

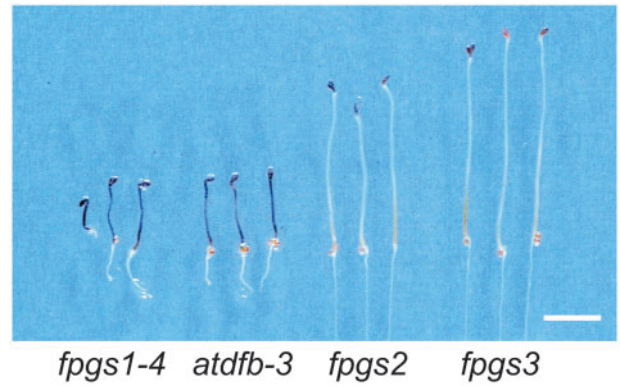

Fig. 4 Starch accumulation in mutants defective for folylpolyglutamate synthetase isozymes. The *fpgs1-4* and *atdfb-3* mutants harbor defects in the same gene, At5g05980, which encodes plastidial folylpolyglutamate synthetase. The *fpgs2* and *fpgs3* mutants are defective in the genes encoding cytosolic (At3g10160) and mitochondrial (At3g55630) isozymes, respectively. Mutants were grown for 5 d in darkness on growth medium containing 60 mM sucrose. Starch accumulation in the seedlings was visualized by iodine staining. Photographs were taken after the seedlings were rearranged on agar plates. Scale bar = 5 mm.

the mutant phenotype were identified for gene mapping. Progeny were scored according to genetic background using a series of molecular genetic markers. As summarized in **Fig. 3A**, gene mapping revealed that the mutation was located close to At5g06250, between At5g05780 and At5g06440.

The Arabidopsis genome sequence was used to design oligonucleotide primers to amplify the At5g05980 gene. Amplified DNA fragments from genomic DNA of *fpgs1-4* and wild-type Arabidopsis were fully sequenced. As indicated in **Fig. 3B**, *fpgs1-4* contained a single nucleotide substitution that changed guanine to adenine at position 639. The substitution occurred in the conserved adenine–guanine motif found at the end of the third intron, suggesting that the substitution had caused alternative transcript splicing to occur. Abnormal splicing was confirmed by comparing cDNA sequences from *fpgs1-4* and wild-type Arabidopsis. The *fpgs1-4* cDNA had a 19 bp deletion at a region corresponding to the start of the fourth exon (red box in **Fig. 3B**). The deletion produced a frameshift of the open reading frame and a premature stop codon in the mutant transcript (**Fig. 3C**).

At5g05980, annotated as *FPGS1*, encodes a plastidial isozyme of FPGS, which catalyzes the addition of a polyglutamate tail to THF at a late stage of folate metabolism in plastids (Ravanel et al. 2001). Several mutant alleles of this gene were identified previously and designated as *fpgs1-1-3*, *atdfb-1-3* and *mko2* (Mehrshahi et al. 2010, Srivastava et al. 2011, Reyes-Hernandez et al. 2014). For example, *atdfb-3* contains a T-DNA insertion within the eighth exon (**Fig. 3B**) (Srivastava et al. 2011). None of the previous studies described a relationship between FPGS1 and starch metabolism. As our mutant constituted a new allele, it was designated *fpgs1-4*.

Starch accumulation in etioplasts is triggered only by plastidial FPGS

Three isogenes encoding FPGS, *FPGS1*, *FPGS2* (At3g10160) and *FPGS3* (At3g55630), were identified previously (Mehrshahi et al 2010). *FPGS1* encodes the plastidial isozyme, whereas *FPGS2* and *FPGS3* encode the mitochondrial and cytosolic isozymes, respectively. Mutants *fpgs1-4* and *atdfb-3* harbored defects in the *FPGS1* gene (**Fig. 3B**). As shown in **Fig. 4**, seedlings of not only *fpgs1-4* but also *atdfb-3* exhibited a dwarf phenotype and accumulated starch in above-ground plant parts when grown on 60 mM sucrose in darkness. Starch accumulation was also

Table 1 Metabolomics analysis of compounds in *fpgs1-4* and wild-type seedlings grown for 5d in darkness

	fpgs1-4	Wild type (μmol g^{-1} FW)
Serine	4.65	0.78
Glycine	0.55	1.37
Adenine	14.8×10^{-3}	0.93×10^{-3}
G6P[a]	1.00	0.37
G1P[b]	41.2×10^{-2}	21.5×10^{-2}
ADP-glucose	1.72×10^{-3}	0.94×10^{-3}

Values are presented as the mean of triplicate biological samples.
[a] Glucose-6-phosphate.
[b] Glucose-1-phosphate.

examined in *fpgs2* and *fpgs3*, which lacked mitochondrial and cytosolic isozymes, respectively. As shown in **Fig. 4**, neither mutant had a phenotype similar to that of the *fpgs1*-deficient mutants, suggesting that the loss of plastidial FPGS, but not of mitochondrial or cytosolic FPGS, triggered sucrose-dependent starch accumulation in plastids.

Etioplast starch accumulation can be suppressed by the addition of active folate derivatives

The At5g05980 mutation suggested that *fpgs1-4* contained reduced amounts of active folate derivatives. Folate derivatives are known to function as coenzymes for several enzymes such as serine hydroxymethyltransferase, which catalyzes interconversion between glycine and serine. Our metabolomics analysis revealed that serine levels were substantially higher in *fpgs1-4* than in wild-type Arabidopsis, while the amount of glycine was lower in *fpgs1-4* than in wild-type Arabidopsis (**Table 1**). These results suggested that serine hydroxymethyltransferase was inactive in *fpgs1-4* as a result of the loss of active folate derivatives.

If the *fpgs1-4* starch accumulation phenotype occurred as a consequence of lack of folate derivatives, then exogenously supplied folate would be expected to rescue the phenotype. To examine this, 200 μM each of several folate derivatives were supplied: folate, THF, 5-formyl-THF and 5-methyl-THF (**Fig. 5**). Of these, exogenously supplied 5-formyl-THF efficiently suppressed the mutant phenotypes of starch accumulation and dwarfism when grown on medium containing sucrose in darkness. A weaker suppression effect on both phenotypes was observed with 5-methyl-THF. No effect was observed when folate or THF were supplied.

Antifolate agents and adenine can trigger starch accumulation in wild-type Arabidopsis

The effects of the antifolate agents methotrexate and 5FU on starch accumulation in wild-type Arabidopsis were assessed (**Fig. 6**). Methotrexate inhibits dihydrofolate reductase, which is involved in folate biosynthesis (Kremer 2004), and 5FU inhibits thymidylate synthase, which requires a folate derivative as a cofactor (Zhao and Goldman 2003). As described above, dark-grown wild-type Arabidopsis did not accumulate starch in darkness even in the presence of exogenously supplied sucrose. However, starch accumulation was apparent upon the addition

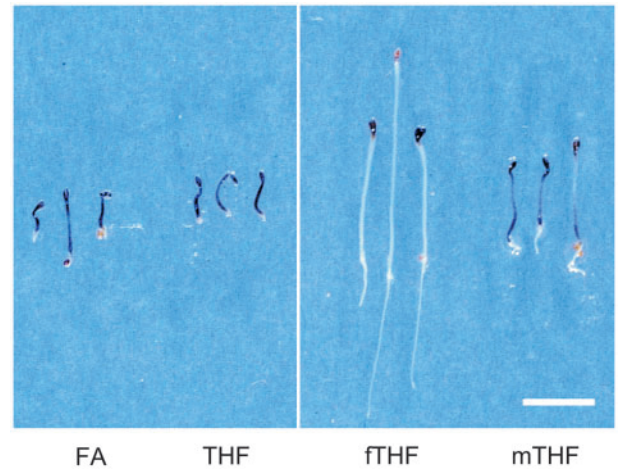

Fig. 5 Abrogation of the *fpgs1-4* phenotype with exogenous folate. The *fpgs1-4* mutant was grown for 5 d in darkness on growth medium containing 200 μM of the folate derivatives indicated at the bottom of the panel. Starch accumulated in the seedlings was visualized by iodine staining. Photographs were taken after the seedlings were rearranged on agar plates. FA, THF, fTHF and mTHF represent folate, tetrahydrofolate, 5-formyl-tetrahydrofolate and 5-methyl-tetrahydrofolate, respectively. Scale bar = 5 mm.

of 0.1 μM methotrexate. Methotrexate also induced a dwarf phenotype in wild-type Arabidopsis. Dwarfism and starch accumulation were also observed when 0.1 mM 5FU was supplied to wild-type Arabidopsis. No such phenotypes were observed when 1 mM uracil was supplied instead of 0.1 mM 5FU (**Fig. 6**). These results suggested that inhibition of thymidylate synthase activity by 5FU was likely to be responsible for the induction of starch accumulation and dwarfism in wild-type plants, and that thymidylate synthase was inactivated in *fpgs1-4* due to loss of its cofactor. Thymidylate synthase is essential for nucleotide biosynthesis, and we therefore reasoned that nucleobase homeostasis might be disordered in *fpgs1-4*. To investigate this possibility, wild-type Arabidopsis was grown in the presence of 1 mM adenine. As shown in **Fig. 6**, dwarfism and starch accumulation were observed in wild-type Arabidopsis supplemented with 1 mM adenine. The phenotypic similarity to *fpgs1-4* suggested a strong link between addition of adenine in wild-type Arabidopsis and loss of active folate in *fpgs1-4* (compare **Fig. 6** with **Fig. 1**). Indeed, our metabolomics analysis revealed that adenine levels were significantly higher in *fpgs1-4* than in wild-type Arabidopsis (**Table 1**).

Folate biosynthesis and starch metabolism are linked

Numerous genes involved in starch metabolism have been identified in Arabidopsis (Streb and Zeeman 2012, Pfister and Zeeman 2016). Of these, *PGM* (At5g51820) encodes plastidial phosphoglucomutase, which is involved in starch biosynthesis, and *SEX4* (starch excess 4, At3g52180) encodes plastidial phosphoglucan phosphatase, which is involved in starch degradation (Caspar et al. 1985, Zeeman et al. 1998). To determine whether *FPGS1* regulated starch biosynthesis or degradation,

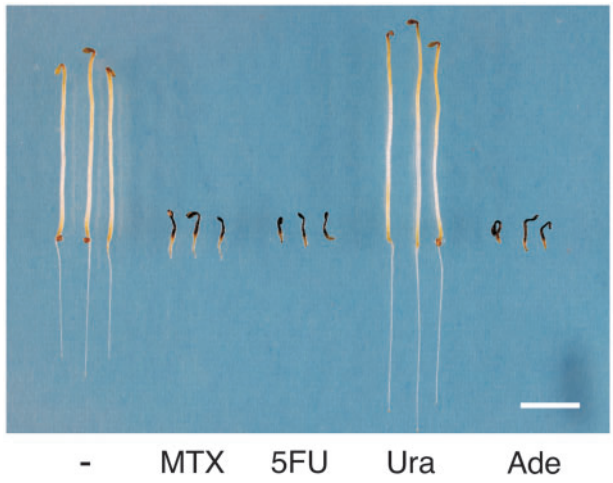

Fig. 6 Effect of antifolates and nucleobases on starch metabolism. Wild-type Arabidopsis seedlings were grown for 5 d under darkness in liquid medium containing 60 mM sucrose alone (−) or together with 100 nM methotrexate (MTX), 0.1 mM 5-fluorouracil (FU), 1 mM uracil (U) or 1 mM adenine (A). Starch accumulated in the seedlings was visualized by iodine staining. Photographs were taken after the seedlings were rearranged on agar plates. Scale bar = 5 mm.

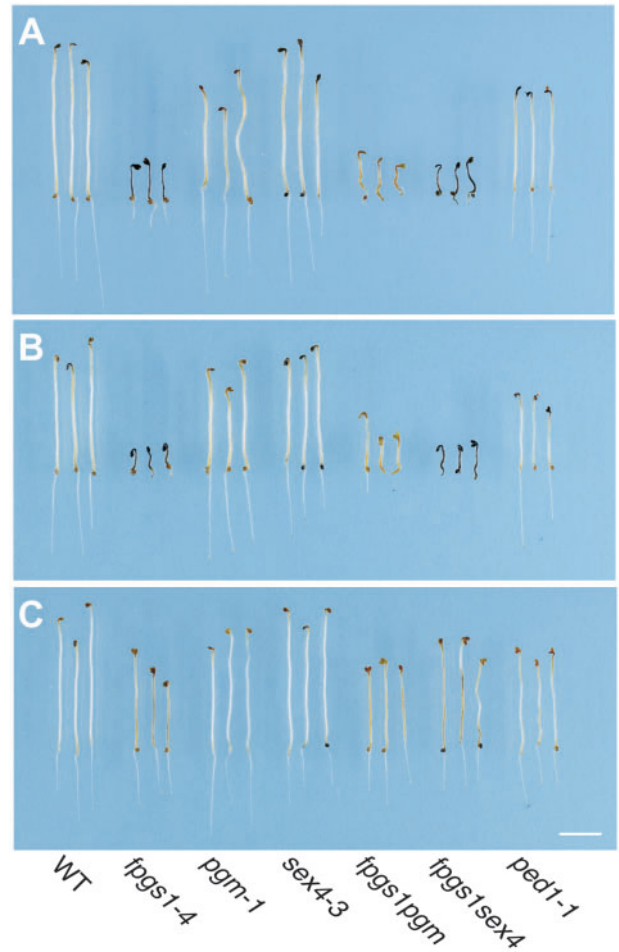

Fig. 7 Mutation of a starch biogenesis gene prevented starch accumulation in *fpgs1-4*. Mutants *pgm-1* and *sex4-3* are defective in starch biosynthesis and degradation, respectively. The mutants were crossed to *fpgs1-4* to establish the double mutants *fpgs1pgm* and *fpgs1sex4*. The mutant *ped1-1*, which is defective in a gene encoding glyoxysomal 3-ketoacyl-CoA thiolase, germinates only when sugar is supplied exogenously. Seedlings were then grown for 5 d in darkness on growth medium containing 60 mM sucrose (A), 120 mM glucose (B) or 120 mM fructose (C). Starch accumulated in the seedlings was visualized by iodine staining. Photographs were taken after the seedlings were rearranged on agar plates. WT, wild-type Arabidopsis. Scale bar = 5 mm.

fpgs1-4 was crossed to the corresponding single mutants, *pgm-1* (Streb et al. 2009) and *sex4-3* (Niittyla et al. 2006), to create two double mutants, *fpgs1pgm* and *fpgs1sex4*. Starch accumulation was examined in the double mutants after cultivation on medium containing 60 mM sucrose (**Fig. 7A**), 120 mM glucose (**Fig. 7B**) or 120 mM fructose (**Fig. 7C**). The single *fpgs1-4* mutant accumulated starch in the presence of glucose as well as sucrose. No starch accumulation was triggered in the *pgm-1* and *sex4-3* mutants under the conditions tested. The double mutant *fpgs1pgm* exhibited similar dwarfism to *fpgs1-4* but did not accumulate starch in the presence of sucrose or glucose (**Fig. 7A, B**). In contrast, *fpgs1sex4* had the same starch accumulation and dwarf phenotypes as *fpgs1-4* (**Fig. 7A, B**). In the presence of fructose (**Fig. 7C**) and mannitol (Supplementary Fig. S1), none of the mutants accumulated starch, and seedlings exhibited elongated hypocotyls similar to those observed in wild-type Arabidopsis. Absorption and utilization of exogenously supplied sugars (sucrose, glucose and fructose) was confirmed by the growth of *ped1-1*. The *ped1-1* mutant is defective in glyoxysomal 3-ketoacyl-CoA thiolase, which is involved in fatty acid β-oxidation, and germinates only when sugar is exogenously supplied (Hayashi et al. 1998b). Indeed, the mutant could germinate on the media containing sucrose, glucose and fructose (**Fig. 7**), but not on the medium containing mannitol (Supplementary Fig. S1), indicating that osmotic stress does not contribute to starch accumulation in *fpgs1-4*.

FPGS1 loss triggers starch accumulation in chloroplasts under darkness in the presence of exogenous sucrose

Chloroplasts are one type of differentiated plastid found in leaf cells. Starch accumulation was assessed in chloroplasts of *fpgs1-4*, *sex4-3*, *fpgs1sex4* and wild-type Arabidopsis in the presence of exogenous sucrose in the dark (**Fig. 8**). All plants accumulated starch in their leaves after cultivation for 2 weeks under constant illumination (**Fig. 8**, **1**). Under these conditions, photosynthetically active chloroplasts synthesized transient starch from photoassimilates. In the dark, however, chloroplasts stopped synthesizing starch due to the loss of photoassimilates, and the transient starch was degraded by *SEX4*-encoded plastidial phosphoglucan phosphatase. Starch that had accumulated in chloroplasts of wild-type Arabidopsis and *fpgs1-4* was no longer apparent after 12 h incubation in darkness (**Fig. 8**, **2**; WT and *fpgs1-4*). In contrast, similarly treated *sex4-3* and *fpgs1sex4* plants retained substantial amounts of starch in their leaves (**Fig. 8**, **2**; *sex4-3* and *fpgs1sex4*), as would be expected in the absence of plastidial phosphoglucan

phosphorylase activity. After dark treatment, leaves were removed from plants and cultured for 72 h in liquid medium in the absence or presence of 60 mM sucrose under dark, aerobic conditions. None of the leaves accumulated starch in the absence of sucrose (**Fig. 8**, **3**). However, leaves cultured in the presence of sucrose accumulated starch (**Fig. 8**, **4**), in a mutation-dependent fashion. Leaves of wild-type Arabidopsis did not accumulate starch, whereas starch biosynthesis was triggered in chloroplasts under dark conditions of both single and double *fpgs1-4* mutants (**Fig. 8**, **4**; *fpgs1-4* and *fpgs1-4sex4*). The *sex4*-5 single mutant contained starch in the apical leaf region (**Fig. 8**, **4**; *sex4*); however, the exogenous sucrose may have inhibited degradation of transient starch.

Discussion

Relationship between plastidial folate and starch biosynthesis

Analyses of the mutant *fpgs1-4* uncovered evidence showing a link between starch metabolism and plastidial FPGS1 (**Figs. 1**, **3**). The *fpgs1-4* mutation resulted in loss of active folate derivatives such as 5-formyl-THF (**Fig. 5**), and induced accumulation of starch granules in etioplasts (**Figs. 1**, **2**) and non-photosynthetic chloroplasts (**Fig. 8**) when plants were cultured in the darkness in the presence of exogenous sucrose. Similar starch accumulation was seen in *atdfb-3*, another allele of *fpgs1*, further supporting the role of plastidial FPGS in starch metabolism (**Fig. 4**). Methotrexate is an antifolate agent that inhibits dihydrofolate reductase, one of the enzymes involved in folate biosynthesis. Inhibition of dihydrofolate reductase would be expected to decrease the amount of active folate derivatives in wild-type seedlings and induce phenotypes identical to *fpgs1-4* (**Fig. 9**). As predicted, exogenously supplied methotrexate induced starch accumulation in etioplasts of wild-type Arabidopsis grown in the presence of sucrose in the dark (**Fig. 6**). Active folate derivatives are synthesized in three different subcellular components: the plastid, mitochondrion and cytosol. However, no starch accumulation was observed in mutants of the mitochondrial and cytosolic isozymes (**Fig. 4**), demonstrating that starch accumulation was driven exclusively by the plastidial folate derivatives. Overall, the results clearly indicated that loss of plastidial folate derivatives induced starch accumulation in non-photosynthetic chloroplasts and etioplasts in the presence of exogenously supplied sucrose in darkness. The relationship between folate and starch accumulation has not been investigated to date (Miret and Munne-Bosch 2014, Colinas and Fitzpatrick 2015). Indeed, several previous studies examined phenotypes of *fpgs1* alleles, but none described starch accumulation in plastids (Mehrshahi et al. 2010, Srivastava et al. 2011, Meng et al. 2014, Reyes-Hernandez et al. 2014, Srivastava et al. 2015). In this study, starch accumulation in non-photosynthetic plastids became apparent only when sucrose was supplied to the plants under darkness. Addition of sucrose provided an unlimited source of precursor for starch biosynthesis, whereas growth in darkness prevented differentiation of etioplasts into chloroplasts and prevented biosynthesis of starch from photoassimilates in chloroplasts.

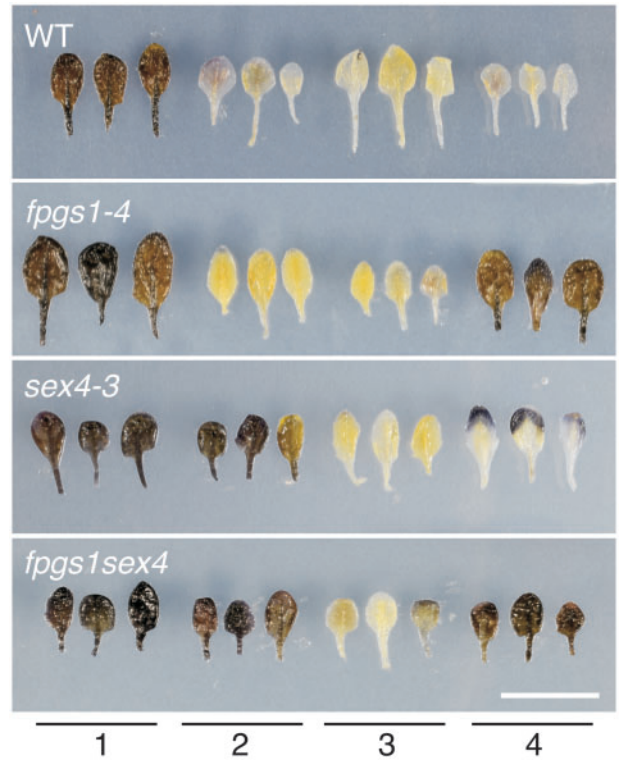

Fig. 8 Leaves of *fpgs1-4* can accumulate starch synthesized from exogenously supplied sucrose under darkness. Wild-type Arabidopsis (WT), *fpgs1-4*, *sex4-3* and the double mutant *fpgs1sex4* were grown for 2 weeks on growth medium containing 60 mM sucrose under constant illumination. Leaves were sampled (1), and the plants were then transferred to darkness. Leaves were removed after 12 h in darkness (2), some of which were cultured for a further 72 h in liquid growth medium without sucrose (3) and with 60 mM sucrose (4). Starch accumulated in leaves was visualized by iodine staining. Photographs were taken after the leaves were rearranged on agar plates. Scale bar = 1 cm.

Non-photosynthetic plastids contain a complete set of enzymes necessary for starch biosynthesis

Plants accumulate two different types of starch: reserved starch and transient starch. Amyloplasts, a type of functionally differentiated plastid, store reserved starch. Amyloplasts are found mainly in cells of sink organs such as cotyledons/endosperm of starchy seeds, tubers and tuberous roots (Tuncel and Okita 2013), all of which contain numerous amyloplasts. Starch biosynthesis in amyloplasts is triggered by the influx of sucrose transported from photosynthetically active source organs, i.e. leaves, into the cells of these sink organs (Comparot-Moss and Denyer 2009). Sucrose is converted to glucose-6-phosphate (G6P) in the cytosol. G6P is then imported into plastids and converted into glucose-1-phosphate (G1P) by phosphoglucomutase (PGM) (see **Fig. 9**). G1P is then conjugated with ATP to make ADP-glucose (ADPG) by the action of ADP-glucose pyrophosphorylase (AGPase). Multiple processes performed by enzymes such as starch synthases (SSs) then polymerize ADPG to produce

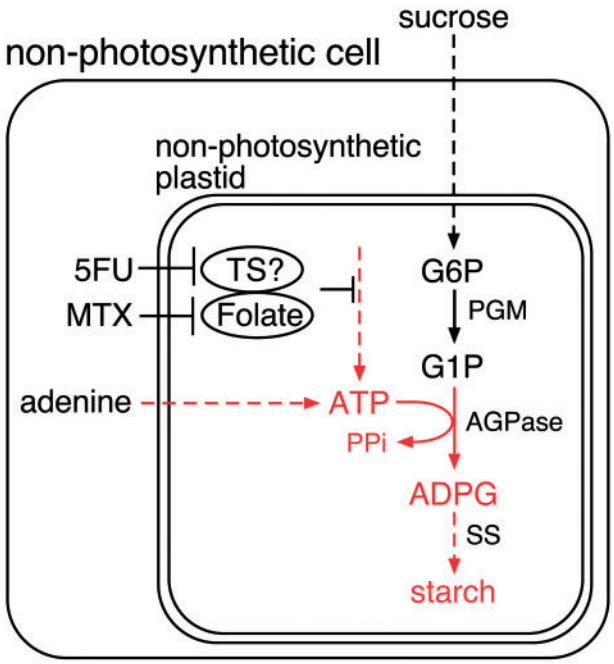

Fig. 9 Schematic illustration showing the relationship between folate and starch biosynthesis in a non-photosynthetic cell. A non-photosynthetic plastid in the cell contains a complete set of enzymes necessary for starch biosynthesis, such as phosphoglucomutase (PGM), ADP-glucose pyrophosphorylase (AGPase) and starch synthase (SS). Glucose-6-phosphate (G6P) imported into the plastid is converted to glucose-1-phosphate (G1P). G1P, however, cannot be metabolized into ADP-glucose (ADPG), since these plastids do not contain enough ATP. ATP production in the non-photosynthetic plastids is suppressed by an enzyme [most probably thymidylate synthase (TS)] that requires active folate as a cofactor. The suppression is released when the enzyme activity is inhibited by 5-fluorouracil (5FU), or when folate biosynthesis is blocked by methotrexate (MTX), or by loss of FPGS1. Exogenously supplied adenine may also induce production of ATP and starch biosynthesis in the presence of G1P. Lines and characters shown in black represent reactions, enzymes and substrates that are present in non-photosynthetic plastids, whereas red represents those that are absent. Solid lines represent a single enzymatic reaction, whereas dotted lines represent multiple reactions.

reserved starch. In contrast, transient starch is formed in chloroplasts of photosynthetically active source organs. Transient starch is synthesized from photoassimilates, i.e. triose phosphate, and is accumulated during the daytime in the presence of sufficiently strong illumination. Reserved starch and transient starch are synthesized from a common precursor, ADPG (Murata et al. 1963, Murata and Akazawa 1964). However, transient starch is degraded at night (Graf and Smith 2011) and non-photosynthetic chloroplasts under dark conditions do not accumulate starch, even in the presence of sucrose (**Fig. 8**). Other plastids, including etioplasts, are not thought to accumulate starch granules. Indeed, etioplasts in dark-grown seedlings of wild-type Arabidopsis never accumulated starch (**Fig. 1**). In this study, however, both etioplasts and non-photosynthetic chloroplasts demonstrated a latent ability to accumulate starch in the darkness that was triggered (as in amyloplasts) by an influx of sucrose into the cells. This ability became visible only when Arabidopsis contained reduced amounts of plastidial folate derivatives, indicating that plastidial folate derivatives suppressed starch accumulation in the non-photosynthetic plastids of wild-type Arabidopsis. It should be noted, however, that no starch accumulation was observed in the roots (**Fig. 1**) or seeds of *fpgs1-4* (see the Results), indicating that the mechanism was not universal for all plastid types.

To accumulate significant amounts of starch granules in plastids without folate, either induction of starch biosynthesis or reduction of starch degradation is required. Three lines of evidence suggested that the former is the case. (i) Seeds of *fpgs1-4* did not contain starch, indicating that starch in seedlings was synthesized de novo. (ii) There was no starch accumulation in *sex4-3* (**Fig. 7**). SEX4 is one of the enzymes involved in starch degradation and, if *fpgs1-4* had reduced the activity of starch degradation, *sex4-3* would be expected to accumulate starch in a similar manner to *fpgs1-4*. (iii) There was no starch accumulation in *fpgs1pgm* (**Fig. 7**), indicating that starch was synthesized by PGM, an enzyme engaged in starch biosynthesis. The involvement of PGM was also supported by the observation that starch biosynthesis occurred with glucose but not fructose (**Fig. 7B, C**).

The lack of starch synthesis in the *fpgs1pgm* double mutant indicated that non-photosynthetic plastids, including etioplasts and chloroplasts under dark conditions, have the potential to synthesize starch using a complete set of starch biosynthesis enzymes involving PGM, AGPase and SS (**Fig. 9**). These non-photosynthetic plastids may import G6P from the cytosol. It has been reported that amyloplasts in cereal endosperm can import ADPG directly from the cytosol via an ADPG transporter (Pozueta-Romero et al. 1999, Cakir et al. 2016). However, this was not the case for the *fpgs1* mutant. Complete loss of starch accumulation in the *fpgs1pgm* double mutant indicated that G6P, rather than ADPG, was transported into these plastids. G6P was then converted into G1P by the action of PGM. G1P, one of two substrates for AGPase, however, cannot be further metabolized into starch despite the existence of AGPase in the non-photosynthetic plastids.

Suppression mechanism of starch biosynthesis by folate in non-photosynthetic plastids

Phenotypes of *fpgs1* mutants were examined in several previous studies, which indicated that plastidial folate played a pivotal role in a variety of biological processes such as development, seed reserve accumulation and lignin biosynthesis (Srivastava et al. 2011, Meng et al. 2014, Reyes-Hernandez et al. 2014, Srivastava et al. 2015). Here, we showed that dark-grown *fpgs1-4* seedlings in the presence of sucrose exhibited shortened hypocotyl/root lengths (**Fig. 1**). A dwarf phenotype was also reported when wild-type Arabidopsis was grown with sucrose together with sulfonamide, an inhibitor for folate biosynthesis, although the authors did not describe the starch content (Stokes et al. 2013). The *fpgs1pgm* double mutant exhibited dwarfism despite not accumulating starch, indicating that the dwarf phenotype of *fpgs1-4* was independent of sugar metabolism involving PGM

(Figs. 7, 9). Pleiotropic phenotypes in the mutant are not unexpected as folate derivatives act as cofactors for a variety of enzymes, each of which might induce a different phenotype. Our data suggest that one such enzyme may regulate starch biosynthesis in non-photosynthetic plastids.

Evidence of a starch biosynthetic regulatory enzyme in non-photosynthetic plastids is provided by the observation that 5FU induced starch biosynthesis in wild-type Arabidopsis (Figs. 6, 9). 5FU is an antifolate agent used for cancer therapy that predominantly inhibits thymidylate synthase in animal cells (Zhao and Goldman 2003). Thymidylate synthase requires 5,10-methylene-THF as a cofactor and converts dUMP into dTMP (Ravanel et al. 2011). Arabidopsis has bifunctional enzymes with thymidylate synthase and dihydrofolate reductase activity (Lazar et al. 1993), and it is possible that 5FU inhibits the plastidial isozyme (Fig. 9). Loss of the enzyme cofactor in the *fpgs1-4* mutant or in wild-type Arabidopsis supplied with methotrexate might also reduce the enzyme activity.

Since thymidylate synthase is involved in nucleotide metabolism, we assumed that reduction of the enzyme activity might disrupt nucleotide homeostasis within the plastids. The idea is supported by the observation that exogenously supplied adenine induced starch biosynthesis in etioplasts of wild-type Arabidopsis (Fig. 6). As discussed above, ADPG is a direct precursor of starch biosynthesis. Increased amounts of adenine might induce excess ATP production, which might lead to accelerated production of ADPG via conjugation of ATP with G1P, a reaction catalyzed by AGPase (Fig. 9). Excess ADPG would then up-regulate starch biosynthesis. Non-photosynthetic plastids of *fpgs1-4* probably accumulated starch because loss of plastidial folate derivatives activated biosynthesis of ATP by a pathway that was independent from photosynthesis. Although plastidial thymidylate synthase is a potential candidate for an enzymatic link between folate derivatives and starch biosynthesis, any link between the enzyme and ATP remains to be elucidated (Fig. 9). Irrespective of the mechanisms involved, overall our results suggest that plastidial folate derivatives in wild-type Arabidopsis may activate enzymes, such as plastidial thymidylate synthase, whose activity reduces ATP levels, thereby suppressing starch biosynthesis in the non-photosynthetic plastids (Fig. 9). Thus, although non-photosynthetic plastids have the latent ability to produce G1P, another substrate for AGPase, from sucrose entering cells, starch accumulation is suppressed in wild-type Arabidopsis.

Sucrose is an important biomolecule that allows long-distance transfer of energy from photosynthetic source organs to distal non-photosynthetic cells. Non-photosynthetic cells then catabolize sucrose as an energy source. Sucrose is also metabolized for storage as starch. Our results showed that exogenous sucrose can be converted and stored as starch in etioplasts and non-photosynthetic chloroplasts when folate is absent. However, cells that convert sucrose to starch fail to obtain energy from the sugar. Suppression of starch biosynthesis is thus needed to maintain carbon homeostasis in cells receiving sucrose from source organs. Our results provide a breakthrough in understanding how non-photosynthetic plastids positively suppress starch biosynthesis from imported sugar.

Materials and Methods

Plant materials and chemicals

Arabidopsis thaliana was grown as described previously (Hayashi et al. 1998b, Hayashi et al. 2000). Seeds were surface-sterilized in a solution containing 2% NaClO and 0.05% Triton X-100, and were sown on growth medium [2.3 mg ml^{-1} Murashige and Skoog (MS) salts (Wako Pure Chemical Industries Ltd.), 100 μg ml^{-1} *myo*-inositol, 1 μg ml^{-1} thiamine-HCl, 0.5 μg ml^{-1} pyridoxine, 0.5 μg ml^{-1} nicotinic acid, 0.5 mg ml^{-1} MES-KOH (pH 5.8) ± 60 mM sucrose] containing 0.8% agar under axenic conditions. Germination was activated by incubation in the dark for 48 h at 4°C, followed by irradiation with white light (100 μE m^{-2} s^{-1}) at 22°C for 6 h. Seedlings were grown at 22°C for 5 d in darkness.

In some experiments, the composition of the growth medium and cultivation conditions were modified as described in the text. For example, when starch accumulation in leaves was examined, plants were grown for 2 weeks under constant illumination, and were then transferred to the dark. After 12 h of dark treatment, leaves were excised from the plants and then vacuum-infiltrated with liquid growth medium (see above) without agar. The leaves were then incubated for 72 h in liquid medium containing 0.02% Silwet L-77 (Bio Medical Science) under vigorous aeration. The same conditions were used for liquid culture of dark-grown seedlings in some experiments.

Ethyl methanesulfonate-mutagenized M_2 seeds of *A. thaliana* accession Columbia were used for mutant screening. Seeds of *atdfb-3* (SALK_015472), *pgm-1* (CS201) and *sex4-3* (SALK_102567C) were provided by the Arabidopsis Biological Resource Center, Ohio State University. *fpgs2* (SALK_008883) and *fpgs3* (SAIL_580_H10) were provided by the Nottingham Arabidopsis Stock Center. cp-GFP, a transgenic Arabidopsis line expressing rbcS–GFP (a fusion protein consisting of an N-terminal transient peptide of RuBisCO small subunit plus GFP) was provided by Dr. Niwa at the University of Shizuoka.

Folate, THF, 5-formyl-THF (folinic acid), methotrexate and 5FU were purchased from Wako Pure Chemical Industires Ltd. and 5-methyl-THF was obtained from Sigma-Aldrich.

Visualization of starch by iodine staining

Starch accumulated in etiolated seedlings and leaves was visualized by iodine staining. Etiolated seedlings grown on agar plates were incubated with 1% iodine solution [1% I2, 1% KI] for approximately 1 min.

Leaves were also incubated with 1% iodine solution for 5 min, and excess iodine was removed by washing with water. Chl in stained leaves was removed by washing with a solution containing 35% chloral hydrate and 6.7% glycerol.

Quantification of starch

Starch content was assayed in seed and seedlings as previously described (Kanai et al. 2007) with minor modifications. Plant tissues were ground with a mortar and pestle in liquid nitrogen, and 5–10 mg of the resulting powder was washed twice with 1 ml of ethanol and twice with 1 ml of distilled water. The precipitate was suspended in 0.2 ml of distilled water and heated in a boiling water bath for 1 h, after which 100 μl of the solution was mixed with an equal volume of 50 mM sodium acetate buffer (pH 5.0). Glucoamylase (50 nkat) (*Rhizopus niveus*; Seikagaku Co.) and 5 nkat α-amylase (Sigma-Aldrich) were then added. The reaction mixture was incubated at 25°C for 1 h, then at 60°C for 1 h. The mixture was then centrifuged at 10,000 × *g* for 10 min, and 100 μl of the supernatant was mixed with 400 μl of a solution containing 60 mM HEPES-KOH (pH 7.4), 5 mM MgCl2, 2 mM NADP and 25 mM ATP. The amount of glucose in the solution was measured by the increase in absorbance at 340 nm after the addition of 1 μl each of hexokinase (2.8 nkat; Sigma-Aldrich) and G6P dehydrogenase (2.3 nkat; Sigma-Aldrich).

Metabolite analysis

Metabolites accumulated in etiolated seedlings were analyzed by capillary electrophoresis–mass spectrometry as previously described (Anegawa et al. 2015). Wild-type and *fpgs1* seedlings (30 mg FW) grown under darkness in the presence of 60 mM sucrose was homogenized in extraction buffer (MeOH :chloroform :H_2O = 1 : 1 : 0.4) and the aqueous layer collected after centrifugation. The aqueous sample was then fractionated by capillary

electrophoresis (Agilent Technologies) and the metabolites in each fraction were analyzed by mass spectrometry (TOF-MS; Agilent Technologies). The migration time and molecular mass of each metabolite were compared with standards. Metabolite amounts were calculated from spectral peak areas.

Cytological analyses

Five-day-old etiolated seedlings were mounted on glass slides. GFP fluorescence was examined using an LSM510 laser scanning confocal microscope equipped with a 488 nm argon laser and a BP 505–550 emission filter (Carl Zeiss). Some of the seedlings were placed in fixative solution [4% (w/v) paraformaldehyde, 1% (w/v) glutaraldehyde, 10% dimethylsulfoxide and 0.06 M sucrose in 0.05 M cacodylate buffer (pH 7.4)]. The samples were then embedded in Epon (Epon 812 resin, TAAB laboratories). Thin sections were stained with 0.05% toluidine solution (citrate-phosphate buffer, pH 7.0) and then with iodine solution, and then analyzed by light microscopy. Ultrathin sections were also prepared from the same specimen and analyzed by electron microscopy as described previously (Hayashi et al. 2002b).

Genetic analyses and map-based cloning

All genetic analyses were conducted using progeny that had been backcrossed twice with wild-type Arabidopsis. For mapping, crosses were made between mutant and wild-type (accession Landsberg *erecta*) plants. Homozygous F_2 seedlings were scored according to their dwarf phenotype. Map-based cloning was conducted as described previously (Hayashi et al. 2000). Primer pairs for two simple sequence length polymorphism (SSLP0 markers (at5g05780 and at5g06250) were as follows: CAAAACAAAGGGTCAAGTCAG and CATAATG CGTATCAAAGCACG, and AAAAACCCAAACTTTCTATTTATAC and ACTTC GCTTCAAGTAAAGAGG, respectively.

A CAPS (cleaved amplified polymorphic sequence) marker (at5g06440) was amplified with GGATCAGTTAAAGCTCTACTG and AAGGATGAAGGTACCA TGGC and then digested with *Dde*I.

DNA sequencing analyses

Genomic DNA was extracted from etiolated seedlings using a DNeasy Plant Mini Kit (Qiagen). TAIR10 [Arabidopsis genome sequence data at the Arabidopsis Information Resource (www.arabidopsis.org)] was used to design primer pairs for amplification of genes at mapping positions. Amplified fragments were sequenced directly as described previously (Hayashi et al. 1998b).

Reverse transcription–PCR (RT–PCR)

RT–PCR was performed as described previously (Kanai et al. 2010). Total RNA was extracted from etiolated seedlings using an RNeasy Plant Mini Kit (Qiagen). cDNA was synthesized from 2 μg of total RNA using Ready-to-GO RT-PCR beads (GE Healthcare). Amplification and sequence determination of cDNA fragments from wild-type Arabidopsis and *fpgs1-4* were performed using the A CCAGCCTCACCTACCATCT and ATGGCTTCATCAGGTTGGGG primer pair, as described above.

Supplementary data

Supplementary data are available at PCP online.

Funding

This work was supported by the Ministry of Education, Science, and Culture of Japam [grants-in-aid for scientific research grant No. 15K07117].

Acknowledgments

We thank the Arabidopsis Biological Resource Center, Nottingham Arabidopsis Stock Center and Dr. Y. Niwa at the University of Shizuoka for providing seeds. We also thank Ms. M. Kondo and all the staff members at Spectrography and Bioimaging Facility, NIBB Core Research Facilities for their support with cytological analysis (No. 15-340), and Ms. Y. Yoshinori at the National Institute for Basic Biology, and Mrs. R. Hirayama and S. Yamamoto at the Nagahama Institute of Bioscience and Technology for their technical support. We dedicate this work to the late Dr. Takashi Akazawa, Professor Emeritus of Nagoya University, who made great contributions to the field of starch metabolism and who supported and encouraged us in our research over many years.

Disclosures

The authors have no conflicts of interest to declare.

References

Anegawa, A., Ohnishi, M., Takagi, D., Miyake, C., Shichijo, C., Ishizaki, K., et al. (2015) Altered levels of primary metabolites in response to exogenous indole-3-acetic acid in wild type and auxin signaling mutants of *Arabidopsis thaliana*: a capillary electrophoresis–mass spectrometry analysis. *Plant Biotechnol.* 32: 65–79.

Cakir, B., Shiraishi, S., Tuncel, A., Matsusaka, H., Satoh, R., Singh, S., et al. (2016) Analysis of the rice ADP-glucose transporter (OsBT1) indicates the presence of regulatory processes in the amyloplast stroma that control ADP-glucose flux into starch. *Plant Physiol.* 170: 1271–1283.

Colinas, M. and Fitzpatrick, T.B. (2015) Natures balancing act: examining biosynthesis *de novo*, recycling and processing damaged vitamin B metabolites. *Curr. Opin. Plant Biol.* 25: 98–106.

Comparot-Moss, S. and Denyer, K. (2009) The evolution of the starch biosynthetic pathway in cereals and other grasses. *J. Exp. Bot.* 60: 2481–2492.

Caspar, T., Huber, S.C., and Somerville, C. (1985) Alterations in Growth, Photosynthesis, and Respiration in a Starchless Mutant of Arabidopsis thaliana (L.) Deficient in Chloroplast Phosphoglucomutase Activity. *Plant Physiol* 79: 11–17.

Eastmond, P.J. (2006) SUGAR-DEPENDENT1 encodes a patatin domain triacylglycerol lipase that initiates storage oil breakdown in germinating Arabidopsis seeds. *Plant Cell* 18: 665–675.

Gerdes, S., Lerma-Ortiz, C., Frelin, O., Seaver, S.M.D., Henry, C.S., de Crecy-Lagard, V., et al. (2012) Plant B vitamin pathways and their compartmentation: a guide for the perplexed. *J. Exp. Bot.* 63: 5379–5395.

Graf, A. and Smith, A.M. (2011) Starch and the clock: the dark side of plant productivity. *Trends Plant Sci.* 16: 169–175.

Hanson, A.D. and Gregory, J.F. (2011) Folate biosynthesis, turnover, and transport in plants. *Annu. Rev. Plant Biol.* 62: 105–125.

Hayashi, M., De Bellis, L., Alpi, A. and Nishimura, M. (1995) Cytosolic aconitase participates in the glyoxylate cycle in etiolated pumpkin cotyledons. *Plant Cell Physiol.* 36: 669–680.

Hayashi, H., De Bellis, L., Ciurli, A., Kondo, M., Hayashi, M. and Nishimura, M. (1999) A novel acyl-CoA oxidase that can oxidize short-chain acyl-CoA in plant peroxisomes. *J. Biol. Chem.* 274: 12715–12721.

Hayashi, H., De Bellis, L., Hayashi, Y., Nito, K., Kato, A., Hayashi, M., et al. (2002a) Molecular characterization of an Arabidopsis acyl-coenzyme A synthetase localized on glyoxysomal membranes. *Plant Physiol.* 130: 2019–2026.

Hayashi, H., DeBellis, L., Yamaguchi, K., Kato, A., Hayashi, M. and Nishimura, M. (1998a) Molecular characterization of a glyoxysomal long chain acyl-CoA oxidase that is synthesized as a precursor of higher molecular mass in pumpkin. *J. Biol. Chem.* 273: 8301–8307.

Hayashi, M., Nito, K., Toriyama-Kato, K., Kondo, M., Yamaya, T., and Nishimura, M. (2000) AtPex14p maintains peroxisomal functions by determining protein targeting to three kinds of plant peroxisomes. *EMBO J.* 19: 5701–5710.

Hayashi, M. and Nishimura, M. (2002) Genetic approaches to understand plant peroxisomes. *In* Plant Peroxisome. Edited by Baker, A. and Graham, I. pp. 279–303. Kluwer Academic Publishers, Dordrecht.

Hayashi, M. and Nishimura, M. (2003) Entering a new era of research on plant peroxisomes. *Curr. Opin. Plant Biol.* 6: 577–582.

Hayashi, M. and Nishimura, M. (2006) *Arabidopsis thaliana*—a model organism to study plant peroxisomes. *Biochim. Biophys. Acta* 1763: 1382–1391.

Hayashi, M., Nito, K., Takei-Hoshi, R., Yagi, M., Kondo, M., Suenaga, A., et al. (2002b) Ped3p is a peroxisomal ATP-binding cassette transporter that might supply substrates for fatty acid β-oxidation. *Plant Cell Physiol.* 43: 1–11.

Hayashi, M., Toriyama, K., Kondo, M. and Nishimura, M. (1998b) 2,4-Dichlorophenoxybutyric acid-resistant mutants of Arabidopsis have defects in glyoxysomal fatty acid β-oxidation. *Plant Cell* 10: 183–195.

Hayashi, Y., Hayashi, M., Hayashi, H., Hara-Nishimura, I. and Nishimura, M. (2001) Direct interaction between glyoxysomes and lipid bodies in cotyledons of the *Arabidopsis thaliana ped1* mutant. *Protoplasma* 218: 83–94.

Kanai, M., Higuchi, K., Hagihara, T., Konishi, T., Ishii, T., Fujita, N., et al. (2007) Common reed produces starch granules at the shoot base in response to salt stress. *New Phytol.* 176: 572–580.

Kanai, M., Nishimura, M. and Hayashi, M. (2010) A peroxisomal ABC transporter promotes seed germination by inducing pectin degradation under the control of ABI5. *Plant J.* 62: 936–947.

Kato, A., Hayashi, M., Mori, H. and Nishimura, M. (1995) Molecular characterization of a glyoxysomal citrate synthase that is synthesized as a precursor of higher molecular mass in pumpkin. *Plant Mol. Biol.* 27: 377–390.

Kato, A., Hayashi, M., Takeuchi, Y. and Nishimura, M. (1996) cDNA cloning and expression of a gene for 3-ketoacyl-CoA thiolase in pumpkin cotyledons. *Plant Mol. Biol.* 31: 843–852.

Kato, A., Takeda-Yoshikawa, Y., Hayashi, M., Kondo, M., Hara-Nishimura, I. and Nishimura, M. (1998) Glyoxysomal malate dehydrogenase in pumpkin: cloning of a cDNA and functional analysis of its presequence. *Plant. Cell Physiol.* 39: 186–195.

Kremer, J.M. (2004) Toward a better understanding of methotrexate. *Arthritis Rheum.* 50: 1370–1382.

Lazar, G., Zhang, H. and Goodman, H.M. (1993) The origin of the bifunctional dihydrofolate reductase–thymidylate synthase isogenes of *Arabidopsis thaliana*. *Plant J.* 3: 657–668.

Mano, S., Hayashi, M., Kondo, M. and Nishimura, M. (1996) cDNA cloning and expression of a gene for isocitrate lyase in pumpkin cotyledons. *Plant Cell Physiol.* 37: 941–948.

Mano, S., Miwa, T., Nishikawa, S., Mimura, T. and Nishimura, M. (2009) Seeing is believing: on the use of image databases for visually exploring plant organelle dynamics. *Plant Cell Physiol.* 50: 2000–2014.

Mehrshahi, P., Gonzalez-Jorge, S., Akhtar, T.A., Ward, J.L., Santoyo-Castelazo, A., Marcus, S.E., et al. (2010) Functional analysis of folate polyglutamylation and its essential role in plant metabolism and development. *Plant J.* 64: 267–279.

Meng, H.Y., Jiang, L., Xu, B.S., Guo, W.Z., Li, J.L., Zhu, X.Q., et al. (2014) Arabidopsis plastidial folylpolyglutamate synthetase is required for seed reserve accumulation and seedling establishment in darkness. *PLos One* 9: e101905.

Miret, J.A. and Munne-Bosch, S. (2014) Plant amino acid-derived vitamins: biosynthesis and function. *Amino Acids* 46: 809–824.

Mori, H. and Nishimura, M. (1989) Glyoxysomal malate synthase is specifically degraded in microbodies during greening of pumpkin cotyledons. *FEBS Lett.* 244: 163–166.

Murata, T. and Akazawa, T. (1964) The role of adenosine diphosphate glucose in leaf starch formation. *Biochem. Biophys. Res. Commun.* 16: 6–11.

Murata, T., Minamikawa, T. and Akazawa, T. (1963) Adenosine diphosphate glucose in rice and its role. *Biochem. Biophys. Res. Commun.* 13: 439–443.

Niittyla, T., Comparot-Moss, S., Lue, W.L., Messerli, G., Trevisan, M., Seymour, M.D.J., et al. (2006) Similar protein phosphatases control starch metabolism in plants and glycogen metabolism in mammals. *J. Biol. Chem.* 281: 11815–11818.

Pfister, B. and Zeeman, S.C. (2016) Formation of starch in plant cells. *Cell. Mol. Life Sci.* 73: 2781–2807.

Pozueta-Romero, J., Perata, P. and Akazawa, T. (1999) Sucrose–starch conversion in heterotrophic tissues of plants. *Crit. Rev. Plant Sci.* 18: 489–525.

Ravanel, S., Cherest, H., Jabrin, S., Grunwald, D., Surdin-Kerjan, Y., Douce, R., et al. (2001) Tetrahydrofolate biosynthesis in plants: molecular and functional characterization of dihydrofolate synthetase and three isoforms of folylpolyglutamate synthetase in *Arabidopsis thaliana*. *Proc. Natl. Acad. Sci. USA* 98: 15360–15365.

Ravanel, S., Douce, R. and Rebeille, F. (2011) Metabolism of folates in plants. *In* Biosynthesis of Vitamins in Plants, Part B. Advances in Botanical Research, Vol. 9. Edited by Rebeille, F. pp. 67–106. Academic Press, London.

Reyes-Hernandez, B.J., Srivastava, A.C., Ugartechea-Chirino, Y., Shishkova, S., Ramos-Parra, P.A., Lira-Ruan, V., et al. (2014) The root indeterminacy-to-determinacy developmental switch is operated through a folate-dependent pathway in *Arabidopsis thaliana*. *New Phytol.* 202: 1223–1236.

Srivastava, A.C., Chen, F., Ray, T., Pattathil, S., Pena, M.J., Avci, U., et al. (2015) Loss of function of folylpolyglutamate synthetase 1 reduces lignin content and improves cell wall digestibility in Arabidopsis. *Biotechnol. Biofuels* 8: 224–240.

Srivastava, A.C., Ramos-Parra, P.A., Bedair, M., Robledo-Hernandez, A.L., Tang, Y.H., Sumner, L.W., et al. (2011) The folylpolyglutamate synthetase plastidial isoform Is required for postembryonic root development in Arabidopsis. *Plant Physiol.* 155: 1237–1251.

Stokes, M.E., Chattopadhyay, A., Wilkins, O., Nambara, E. and Campbell, M.M. (2013) Interplay between sucrose and folate modulates auxin signaling in Arabidopsis. *Plant Physiol.* 162: 1552–1565.

Streb, S., Egli, B., Eicke, S. and Zeeman, S.C. (2009) The debate on the pathway of starch synthesis: a closer look at low-starch mutants lacking plastidial phosphoglucomutase supports the chloroplast-localized pathway. *Plant Physiol.* 151: 1769–1772.

Streb, S. and Zeeman, S.C. (2012) Starch metabolism in Arabidopsis. *Arabidopsis Book* 10: e0160.

Theodoulou, F.L. and Eastmond, P.J. (2012) Seed storage oil catabolism: a story of give and take. *Curr. Opin. Plant Biol.* 15: 322–328.

Tuncel, A. and Okita, T.W. (2013) Improving starch yield in cereals by overexpression of ADPglucose pyrophosphorylase: expectations and unanticipated outcomes. *Plant Sci.* 211: 52–60.

Zeeman, S.C., Smith, S.M., and Smith, A.M. (2007) The diurnal metabolism of leaf starch. *Biochem. J.* 401: 13–28.

Zhao, R.B. and Goldman, I.D. (2003) Resistance to antifolates. *Oncogene* 22: 7431–7457.